

# Field-dependent thermoelectric power and thermal conductivity in multilayered and granular giant magnetoresistive systems

Jing Shi\*

*Department of Physics, University of California, Santa Barbara, California 93106*

Kevin Pettit<sup>†</sup>

*Department of Physics, University of Illinois, Urbana, Illinois 61801*

E. Kita

*Institute of Applied Physics, University of Tsukuba, Tsukuba, Ibaraki 305, Japan*

S. S. P. Parkin

*IBM Almaden Research Center, San Jose, California 95120-6099*

R. Nakatani

*Central Research Laboratory, Hitachi Ltd., Kokubunji, Tokyo 185, Japan*

M. B. Salamon

*Department of Physics, University of Illinois, Urbana, Illinois 61801*

(Received 28 June 1996)

The giant magnetoresistance (GMR) effect in granular and multilayer thin films has been widely investigated because of possible device applications. Despite this intensive effort, the underlying mechanisms responsible for the effect have not been identified. We present measurements of the thermoelectric power (TEP) and thermal conductivity on a wide variety of granular and multilayer GMR systems. The strong magnetic field dependences of both the TEP and the thermal conductivity are found to be closely related to the magnetoresistance. The TEP measurements require that the high density of states in the ferromagnetic materials play a major role in the GMR effect. The thermal conductivity measurements indicate that the scattering mechanisms in granular samples are elastic while multilayer samples have a significant inelastic, spin-flip component. [S0163-1829(96)09745-7]

## I. INTRODUCTION

Nanoscale metallic ferromagnets, in the form of thin layers and single-domain particles, when separated by nonmagnetic metals, can exhibit remarkable changes in electrical resistance as they magnetize.<sup>1</sup> This so-called giant magnetoresistance (GMR) effect has been widely studied and is currently finding applications.<sup>2</sup> Despite this intensive effort, however, the underlying mechanisms responsible for the effect, whether in layered systems or granular materials, have not been positively identified. It is our assertion that, by focusing on the GMR effect itself and ignoring the changes in other transport properties, researchers have missed essential information that narrows the range of possible mechanisms. In particular, the thermoelectric power,<sup>3-7</sup> and thermal conductivity<sup>8,9</sup> both show “giant” changes; we will refer to these effects as giant magnetothermoelectric power (GMTEP) and giant magnetothermal resistance (GMTR) in the course of this paper.

Essentially all theories of the GMR posit two conduction channels for spin-up and spin-down electrons and downplay spin-flip scattering.<sup>10</sup> At one extreme, models considered heretofore have focused on elastic scattering at the interfaces of planar structures, with a potential of the form<sup>11</sup>

$$V(\hat{\sigma}) = \sum (V_i + J\hat{\sigma} \cdot \hat{M}_i) \delta(z - z_i), \quad (1)$$

where  $V_i$  is the potential at the  $i$ th interface arising from difference in the work functions of the two metals,  $J$  is the  $s$ - $d$  exchange energy,  $\hat{\sigma}$  is the conduction electron spin direction, and  $\hat{M}_i$  is a unit vector in the direction of the magnetization of the ferromagnet at the  $i$ th interface. The interface is located at  $z_i$  and the coefficients  $V$  and  $J$  contain information on interface roughness. When two interfaces are separated by a distance less than the conduction electron's spin-flip mean free path, the potential experienced by the electron is different when the  $\hat{M}_i$  are parallel from when they are oppositely aligned. At the simplest level, the scattering rate can be calculated from Fermi's golden rule, and it is usually assumed that the density of states (DOS) is constant throughout the multilayer structure. At the other extreme, some models<sup>12</sup> exploit the difference between the spin-up and spin-down DOS in the transition metals, but the interfaces are ignored and it is assumed that the GMR effects arise only from the differences in the bulk resistivities of the spin bands of the constituent ferromagnet. It is difficult to see how to extend models of the latter type to granular materials. Furthermore, the size of the GMR effect has been shown to depend on the magnetic material near the interface, rather than that which lies deeper within the magnetic block.<sup>13</sup> Moreover, the thickness of the magnetic layers is typically of order 1 nm, less than the mean free path in the bulk material.

We will argue that the band structure in the vicinity of the interface plays the central role. Each of these models has been refined to account for scattering within the nonmagnetic layer and for spin-flip scattering, but the essential elements remain.<sup>2</sup>

Our goal is to present data on the GMTEP and GMTR effects in a variety of multilayered and granular samples. We will argue that, while the interface scattering picture adequately explains the data, the density of final states rather than the spin dependence of the interfacial potentials is the key factor in producing the magnetotransport effects. One major finding is that the thermoelectric power  $S(H, T)$  of all systems studied obeys the simple relation  $S(H, T) \propto 1/\rho(H, T)$  as the field is varied, where  $\rho(H, T)$  is the sample resistivity. This is similar in form to the familiar Nordheim-Gorter rule,<sup>14</sup> but gives much larger effects. We demonstrated in earlier work on granular systems<sup>15</sup> and multilayers<sup>6</sup> that such dependence follows from the usual Mott formula for the thermoelectric coefficient. In fact, our approach is simply an extension of Mott's arguments as to the source of electrical resistance in transition metals.<sup>16</sup>

The thermal conductivity of both granular and multilayered systems also varies with the resistance, as expected from the Wiedemann-Franz (WF) law. In the case of granular materials, the WF law holds over a broad temperature range, indicating, as is frequently assumed, that the scattering processes are primarily elastic. However, multilayer samples do *not* obey the WF law: The effective Lorentz number is field and temperature dependent. This suggests that the scattering processes which contribute to the GMR in layered systems have a significant inelastic component. We will discuss this in terms of low-energy spin-wave excitations that are present in multilayers, but absent in nanoscale magnetic particles.

In Sec. II we will briefly review the theory of the GMR effect and extend it to include the GMTEP and GMTR effects. Section III describes our experimental techniques and Sec. IV describes the close relationship between the GMTEP and GMR effects in a wide variety of materials. We demonstrate in Sec. V how our results on GMTR reveal fundamental differences between the scattering processes at work in granular and multilayer systems and finally, in Sec. VI, discuss our results in light of the existing theories of GMR.

## II. MAGNETOTRANSPORT THEORIES

Giant magnetoresistance was first discovered in antiferromagnetically coupled Fe layers separated by Cr spacers.<sup>1</sup> The MR ratio was defined as

$$\mathcal{R} = \frac{\rho_{AF^-} - \rho_F}{\rho_{AF}}, \quad (2)$$

which approaches unity if the resistivity  $\rho_F$  in the ferromagnetic state is much smaller than the resistivity in the antiferromagnetic or unmagnetized state  $\rho_{AF}$ . There has been an unfortunate tendency to substitute  $\rho_F$  for  $\rho_{AF}$  in the denominator, thereby inflating the value of  $\mathcal{R}$ . Subsequent research demonstrated that  $\mathcal{R}$  oscillates with the thickness of the nonmagnetic spacer layer in a large number of multilayer systems based on Fe, Co, and Permalloy magnetic layers separated by various nonmagnetic metals.<sup>17,18</sup> Antiferromagnetic

coupling is not essential: GMR has been observed in systems composed of uncoupled magnetic granules;<sup>19</sup> the construction of novel structures with uncoupled, pinned, or biased ferromagnetic layers that exhibit the GMR effect has been termed "spin engineering."

As noted above, theories of this effect have built on the two-current model of Fert and Campbell.<sup>20</sup> Separate resistivities  $\rho_\uparrow$  and  $\rho_\downarrow$  are defined for each spin channel and an asymmetry parameter  $\alpha = \rho_\downarrow/\rho_\uparrow$  is introduced. Here, "up" and "down" refer to the *local* magnetization direction for each magnetic layer or granule. The global quantization axis is defined by the external field and can be denoted by subscripts + and -. If spin-flip and bulk scattering are ignored, it is straightforward to show,<sup>10,2</sup> by projecting the up and down components of the + and - spin polarizations at successive interfaces, that

$$\rho_F = \frac{\rho_\uparrow \rho_\downarrow}{(\rho_\downarrow + \rho_\uparrow)} = \frac{\alpha \rho_\uparrow}{(1 + \alpha)} \quad (3)$$

and

$$\rho_{AF} = \frac{(\rho_\downarrow + \rho_\uparrow)}{4} = \frac{(1 + \alpha)\rho_\uparrow}{4}. \quad (4)$$

This leads to

$$\mathcal{R} = \left( \frac{\alpha - 1}{\alpha + 1} \right)^2. \quad (5)$$

The problem is then to determine the asymmetry parameter  $\alpha$  for a particular model. Using the Kubo formalism, Levy, Zhang, and Fert<sup>11</sup> (LZF) calculated  $\alpha$  under the assumption that the electronic structure, i.e., the DOS, is constant throughout the sample. This would best apply if conduction takes place in the *s* bands and if *s*→*d* scattering is unimportant. When bulk scattering can be ignored in favor of interface scattering, the asymmetry parameter can be written as

$$\alpha = \left( \frac{V + J}{V - J} \right)^2. \quad (6)$$

Note that in the absence of a spin-independent potential *V*,  $\alpha$  is unity and the MR ratio vanishes. LZF obtain satisfactory values of  $\mathcal{R}$  for an Fe/Cr multilayer using  $J/V \approx 0.5$ . As a consequence of the assumption of a common DOS for both spin channels throughout the structure, the asymmetry parameter is a constant, arising solely from the ratio of spin-dependent and spin-independent matrix elements.

Exactly the opposite point of view has been adopted by Edwards and Mathon.<sup>12</sup> They base their analysis on Mott scattering within the bulk ferromagnetic layer where the high DOS at the Fermi energy in the *d* bands causes *s*→*d* scattering processes to dominate the resistivity. Interfacial scattering is ignored and the resistivity is calculated from parallel and series connections of resistors representing the spacer and magnetic layers. The asymmetry ratio then refers to the low- and high-resistivity channels  $\rho_M^L$  and  $\rho_M^H$  within the magnetic layers. In the limit that the resistivities of both spin channels in the magnetic metal are much larger than that of the spacer, the MR ratio is again given by Eq. (5), with

$\alpha = \rho_M^H / \rho_M^L$ . In Mott scattering, the  $s$ -band resistivity is proportional to the  $d$ -band DOS. Here, one spin subband is assumed to have a high DOS at the Fermi level  $g_H(E_F)$  and the other a low DOS  $g_L(E_F)$ ; hence  $\alpha = g_H(E_F) / g_L(E_F)$ . Edwards and Mathon ascribe the decrease in the MR ratio with increasing spacer thickness to the short-circuiting effect of the spacer; in the LZF model, however, it is attributed to the effective decoupling of the layers as the spacer-layer thickness and electron mean free path become comparable.

While both models explain the resistivity data they differ fundamentally. In the LZF picture,  $\alpha$  is a constant, determined only by the relative magnitudes of the contact potential and the  $s$ - $d$  exchange constant, while in the Mott picture,  $\alpha$  is determined by the spin-dependent DOS in the ferromagnetic metal. The correct approach cannot be unambiguously distinguished from the resistivity data alone. However, the models predict different behavior for other transport properties, particularly the thermoelectric coefficient.

In metals the diffusion thermoelectric power (TEP) is calculated through the Mott formula<sup>21</sup>

$$S = - \frac{\pi^2 k_B^2 T}{3e} \left( \frac{\partial \ln \sigma(E)}{\partial E} \right)_{E_F}. \quad (7)$$

From Eqs. (3) and (4), one can show that

$$S_{AF} = \frac{\pi^2 k_B^2 T}{3e} \left( \frac{\alpha'}{(1+\alpha)} + \frac{\rho'_\uparrow}{\rho_\uparrow} \right)_{E_F}, \quad (8a)$$

$$S_F = \frac{\pi^2 k_B^2 T}{3e} \left( \frac{\alpha'}{\alpha(1+\alpha)} + \frac{\rho'_\uparrow}{\rho_\uparrow} \right)_{E_F}. \quad (8b)$$

Here,  $\alpha' = \partial \alpha(E) / \partial E$  and  $\rho'_\uparrow = \partial \rho_\uparrow(E) / \partial E$ . Clearly, if the asymmetry ratio is independent of energy, as it is in the LZF model, the TEP is the same in both ferromagnetic and antiferromagnetic states; there is no GMTEP. However, when the asymmetry ratio is energy dependent, we have

$$\Delta S \equiv S_{AF} - S_F = \frac{\pi^2 k_B^2 T}{3e} \frac{\alpha'}{\alpha} \mathcal{R}^{1/2}. \quad (9)$$

The GMTEP depends on the square root of the MR ratio and on the existence of an energy-dependent asymmetry.

As a GMR system is magnetized, the resistivity and other transport properties switch from their antiferromagnetic (or unmagnetized) to their ferromagnetic (or magnetized) values by means of a control function  $f(H, T)$ . In antiferromagnetically coupled multilayers with no anisotropy<sup>11</sup> and in granular systems with a uniform particle size,<sup>15</sup> the control function is closely related to the magnetization through  $f(H, T) = [M(H, T) / M(\infty, T)]^2$ . In general, we can write

$$\rho(H, T) = \rho_{AF} [1 - f(H, T)] + \rho_F f(H, T), \quad (10)$$

and, setting  $\partial \ln f(H, T) / \partial E = 0$ , we arrive at the very useful expression<sup>6</sup>

$$S(H, T) = S_{AF} + \frac{\Delta S (1 - \mathcal{R})}{\mathcal{R}} \left( 1 - \frac{\rho_{AF}}{\rho(H, T)} \right). \quad (11)$$

The inverse relationship between the thermoelectric power and the resistivity is a key result of this analysis. As we show in Sec. IV, this relationship is obeyed by a wide variety of GMR systems, both multilayer and granular.

If the scattering mechanisms that give rise to the GMR and GMTEP are elastic, the WF law will hold with a ratio close to the classical Lorentz number,

$$\kappa_e(H, T) / T \sigma(H, T) = L_0 \equiv 2.45 \times 10^{-8} \text{ W}\Omega/\text{K}^2. \quad (12)$$

Here,  $\kappa_e(H, T)$  is the electronic contribution to the thermal conductivity and  $\sigma(H, T)$  is the electrical conductivity. In pure metals, Eq. (12) holds at temperatures well above the Debye temperature, where large-angle scattering processes predominate, and at low temperatures, where the relaxation rate is determined by impurity and/or boundary scattering. Inelastic, low-angle scattering predominates at intermediate temperatures, causing the WF ratio to fall significantly below  $L_0$ .<sup>21</sup> With increasing impurity content, the WF ratio approaches the Lorentz number over the accessible temperature range.

Early treatments of the GMR neglected spin-mixing processes which, because they require the creation or absorption of a magnon, are inelastic.<sup>22</sup> However, it is well known that the WF ratio of ferromagnetic metals drops precipitously below the Curie temperature.<sup>23</sup> In earlier work, Colquitt<sup>24,25</sup> demonstrated that the rapid decrease in thermal conductivity with temperature is the consequence of inelastic  $s$ - $d$  scattering by magnons. Presumably, the WF ratio decreases with temperature because magnon creation reduces the thermal current more effectively than the electrical current. We will show, in Sec. V, that the thermal conductivity of granular materials satisfies the WF law with a ratio close to  $L_0$ , while for multilayer systems, which can support long-wavelength spin waves, the WF law is not obeyed.

### III. EXPERIMENT

Both multilayer (primarily Co/Cu) and granular (primarily AgCo) samples were used in these studies. Several other combinations of magnetic and nonmagnetic materials were examined to test the generality of the results reported here. Copper-cobalt multilayers were grown at IBM by dc magnetron sputtering by methods described previously.<sup>26</sup> The structures for thermoelectric measurements had the form glass/Fe(50 Å)/[Co(10 Å)/Cu( $t$ )]<sub>39</sub>Co(10 Å)/Fe(25 Å). Four such multilayers were prepared with  $t = 8.3$  Å, 9.2 Å, 17.5 Å, and 19.3 Å; these were chosen to be close to the first and second peaks in the GMR.<sup>27</sup> We abbreviate these as [Co(10 Å)/Cu( $t$ )]<sub>g</sub> to denote the glass substrate. A second set of samples was prepared similarly, with 16 Å of either Cu<sub>63</sub>Ni<sub>37</sub> or Cu<sub>58</sub>Ni<sub>42</sub> as the spacer layer. The former sample has a magnetoresistance ratio that decreases with temperature, but remains observable at 5 K, while the GMR of the latter sample vanishes near 100 K.<sup>28</sup> Three samples of Permalloy/copper were grown at Hitachi Research Laboratories, by methods described elsewhere,<sup>29</sup> with Cu spacer layers 10, 16, and 20 Å thick, separating 10 Å layers of Ni<sub>0.8</sub>Fe<sub>0.2</sub>. These also were grown on a 50 Å Fe buffer and contained 20 bilayers. Two Fe/Cr multilayer samples were grown by dc magnetron sputtering on water-cooled cover glass substrates. The Fe layers were 5 Å and 50 Å thick

while the Cr thickness of 20 Å was chosen to correspond to ferromagnetic coupling between the Fe layers. Magnetic, x-ray, and Mössbauer analysis reveals that the sample with the thinner Fe layers is composed of small Fe islands which are superparamagnetic. We call this a granular multilayer.

Granular samples of AgCo were grown at Illinois by means of dc magnetron cosputtering. Co and Ag were sputtered simultaneously from separate guns at an Ar pressure of  $5 \times 10^{-3}$  torr while the substrates were rotated past each gun at  $\approx 36$  rpm. The sputtering rates of the two guns were adjusted to achieve a composition corresponding to 20 vol. % Co. Cover glass substrates (75  $\mu\text{m}$  thick) were held near room temperature and the final films were 5000 Å thick. After annealing at 300 °C for 10 min, the samples showed Curie law behavior from room temperature to  $\approx 70$  K, which we identify as the blocking temperature. An analysis of the magnetization curves above the blocking temperature could be fit with a single Langevin function corresponding to 980 Co atoms/particle (assuming  $1.6\mu_B$  per Co atom) or approximately 27 Å in diameter. Granular MgFe films were grown by coevaporation under ultrahigh vacuum onto thin glass substrates. The Fe concentration was 20 vol. %. The samples were superparamagnetic, but had a distribution of particle sizes. A more complete description of the growth, characterization, and magnetoresistance of the MgFe samples is available elsewhere.<sup>30</sup>

Thermopower measurements were performed on narrow strips of the sample (typically  $10 \times 2$  mm<sup>2</sup>) using standard methods. The counterelectrodes were either Au or Pb fine wires placed in close contact with a pair of fine (25  $\mu\text{m}$ ) type-E thermocouples. Current leads were placed outside the region between the thermocouples, so that resistance and TEP data could be taken in sequence at each field-temperature point. At all fields the contribution of the voltage leads to the measured TEP was subtracted off using published zero-field values for the TEP of Au or Pb.<sup>31</sup>

While the samples for thermoelectric and resistivity measurements could be grown on glass substrates, a special effort was required to reduce the substrate thermal conductance on the thermal conductivity specimens. Early multilayer work maintained a constant heat current across a thick (6000 Å) sample grown on a thick substrate and monitored the field-dependent change in temperature gradient.<sup>8</sup> Thick granular films were removed from their backing for measurement.<sup>9</sup> For our thermal conductivity measurements, new multilayer Co/Cu samples were grown on low-thermal-conductivity (0.1 W/m K), 13- $\mu\text{m}$  Kapton film with the same sequence as those grown on glass. In this case, spacer layer thicknesses of 10 Å and 23 Å were grown; the inter-layer coupling strength and MR ratio were unaffected by the Kapton substrate. These will be denoted [Co(10 Å)/Cu( $t$  Å)]<sub>K</sub>, with the subscript referring to the Kapton substrate. Even for multilayer films no thicker than 800 Å, the Kapton contributes only  $\approx 15\%$  to the total thermal conductance. Granular AgCo samples were also grown on Kapton substrates in the same manner as above but in this case the concentration was approximately 28 vol. % Co and the samples were not annealed after growth.

Heat loss through electrical leads to the heater and through the thermocouples was reduced to negligible levels by using long lengths of 13  $\mu\text{m}$  wires for Constantan voltage

leads and type-E thermocouples. Radiation loss from the sample was minimized by reducing the sample area and by cementing the exposed Kapton of two segments together so that the low-emissivity metal films faced outward. Despite these precautions, the background thermal conductivity significantly exceeds the nominal conductivity of the Kapton. We focus, therefore, only on the field-dependent part, which is due solely to the samples. To measure the thermal conductivity, a measured power was applied to a microchip resistor used as a heater and the temperature rise ( $\leq 1$  K) was measured through the differential thermocouple by a Keithly 152B voltmeter. Several sequences of heating and cooling were averaged at each field and temperature. Because current and voltage leads would add prohibitively to the heat leak, segments of the same sample were mounted adjacent to the thermal conductivity experiment so that the resistance could be measured at the same field and temperature.

#### IV. MAGNETOTHERMOPOWER

In general, the thermoelectric coefficients of metals do not depend strongly on fields for temperatures greater than 10% of the Debye temperature.<sup>32</sup> Consequently, a large field dependence of the thermopower is even more anomalous than large changes in resistance, particularly at ordinary temperatures. We will restrict our analysis to temperatures above 100 K to avoid phonon drag contributions. Figure 1(a) shows the field dependence of the thermopower  $S$  and the resistance  $R$  for [Co(10 Å)/Cu(8.3 Å)]<sub>g</sub> at 293 K.<sup>6</sup> The thermopower saturates at  $-25.5$   $\mu\text{V/K}$ , comparable to that of elemental Co, and much larger than that of Cu (1.8  $\mu\text{V/K}$ ). The change is  $\Delta S = 6.7$   $\mu\text{V/K}$  and, as shown in Fig. 1(b), the data satisfy Eq. (11) accurately. The slope of the curve is proportional to  $\Delta S$  and, as demonstrated in the inset to Fig. 1(b), exhibits the linear temperature dependence predicted by Eq. (9); changes in  $\rho_{AF}$  are of order 1% over this temperature range. Figure 1(b) also shows the data at 120 K. Note that our definition of  $\Delta S$  differs in sign from that of Piraux *et al.*<sup>5</sup> and that our data are in rough agreement with theirs. The linear relation between thermopower and conductance is a general property of the multilayer samples studied. Similar plots of data taken at room temperature are shown for Ni<sub>81</sub>Fe<sub>19</sub>(10 Å)/Cu(10 Å), Co(10 Å)/Cu<sub>58</sub>Ni<sub>42</sub>(16 Å) [Fig. 2(a)],<sup>33</sup> [Co(10 Å)/Cu(17.5 Å)]<sub>g</sub> [Fig. 2(b)], and [Fe(50 Å)/Cr(20 Å)] [Fig. 2(c)]. We note that the data for Fe/Cr are difficult to interpret for reasons described in Sec. VI A.

Quite similar results have been obtained on granular samples.<sup>34,9</sup> A representative plot of the thermoelectric power versus the conductance for a AgCo granular sample is shown in Fig. 3. Clearly, both the initial and saturated values of  $S$  are considerably smaller than for multilayers. Analogous effects have been observed for other granular materials. Figure 4(a) shows a plot of the thermoelectric power vs the conductance of the granular MgFe film at 300 K, while Figure 4(b) shows a similar plot for the Fe(5 Å)/Cr(20 Å) granular multilayer.

In the discussion leading to Eq. (9) we showed that  $\Delta S$  is determined by the energy dependence of the asymmetry ratio. In a simple Born-approximation picture of interfacial scattering, we suggest that the asymmetry is dominated by the spin-split DOS in the ferromagnetic material, i.e.,

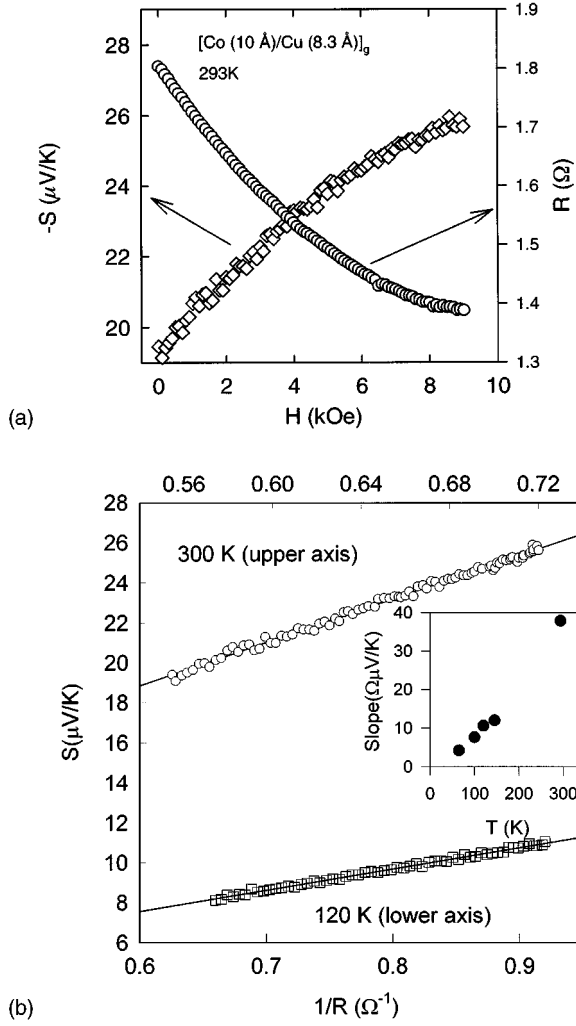


FIG. 1. (a) Resistance and thermoelectric power of the Co/Cu multilayer at 293 K vs field applied in the plane of the sample. (b) The thermopower vs conductance with field as an implicit variable at 300 K and 120 K. The inset shows the temperature dependence of the slope of such plots.

$$\alpha = g_{\downarrow}(E_F)/g_{\uparrow}(E_F), \quad (13a)$$

where  $g_{\uparrow,\downarrow}(E)$  is the final DOS for scattering processes involving up- and down-spin electrons, respectively. Similar, but distinct, conclusions have been reached by Inoue *et al.*,<sup>35</sup> who argue that the relevant densities of states are associated with localized impurity moments within the spacer layer. However, as the definitions of up and down spins are tied to the magnetic layers or granules, we assert that these should properly be considered the DOS of the magnetic layers or granules near the interfaces, making this an extension of the usual Mott picture for the resistivity of transition metals. The necessary quantity is

$$\alpha'/\alpha = g'_{\downarrow}(E_F)/g_{\downarrow}(E_F) - g'_{\uparrow}(E_F)/g_{\uparrow}(E_F). \quad (13b)$$

The minority and majority spin thermoelectric coefficients for Co have been determined by Cadeville and Roussel<sup>36</sup> from which we obtain  $g'_{\uparrow}(E_F)/g_{\uparrow}(E_F) = -4.1 \text{ eV}^{-1}$  and  $g'_{\downarrow}(E_F)/g_{\downarrow}(E_F) = -1.6 \text{ eV}^{-1}$ , giving a value  $\alpha'/\alpha = 2.5$

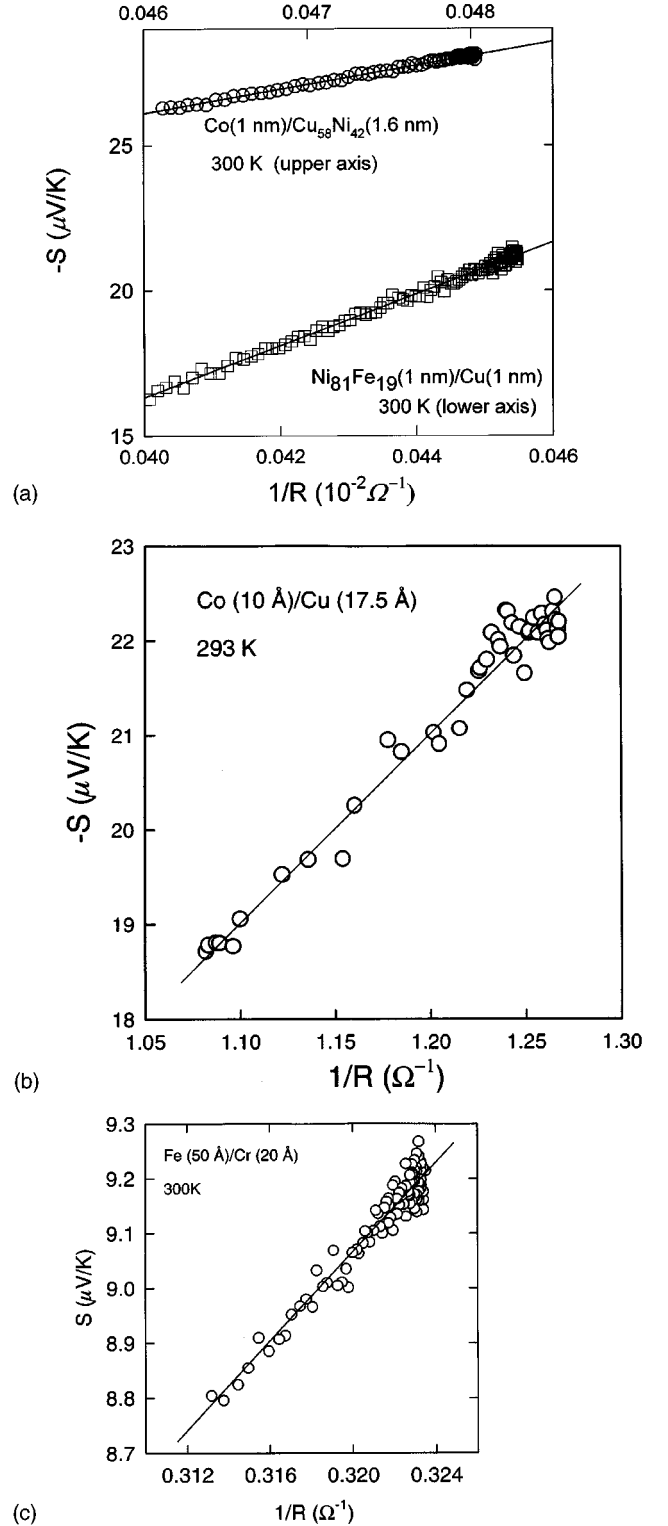


FIG. 2. Plots of the thermoelectric power vs the inverse of the resistance for multilayers of (a) Permalloy/copper and Co/Cu-Ni, (b) Co/Cu at the second antiferromagnetic peak, and (c) Fe/Cr. All data were taken at room temperature.

$\text{eV}^{-1}$ . Application of Eq. (9) to the data of Fig. 1(a) results in a value  $\alpha'/\alpha = 1.9 \text{ eV}^{-1}$ , reasonably close to elemental Co.

In applying Eq. (9) to granular materials, we have ignored the resistivity  $\rho_m$  of the matrix. To include it, we define

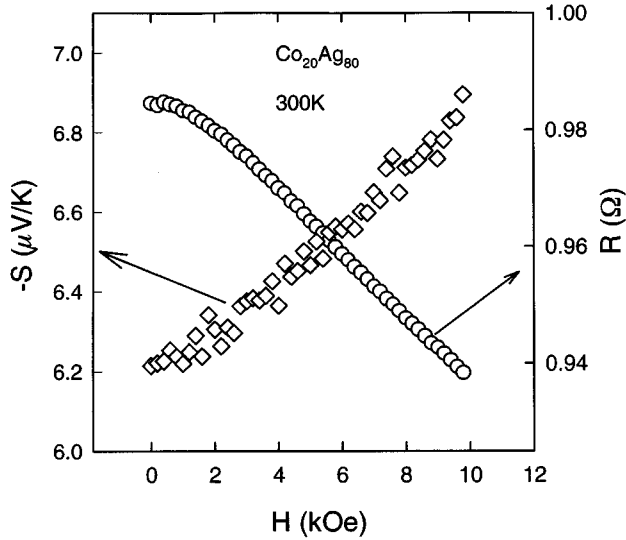


FIG. 3. Thermopower and resistivity of a granular AgCo sample.

$S_{\uparrow,\downarrow} = (\pi^2 k_B^2 T / 3e) g'_{\uparrow,\downarrow}(E_F) / g_{\uparrow,\downarrow}(E_F)$  and apply the usual Nordheim-Gorter rule in the  $H=0$  (demagnetized) state to give

$$S_{AF} = (S_{\uparrow} + S_{\downarrow}) \frac{1 - \beta}{2} + (S_{\uparrow} - S_{\downarrow}) \frac{\sqrt{\mathcal{R}}}{2} + \beta S_0, \quad (14)$$

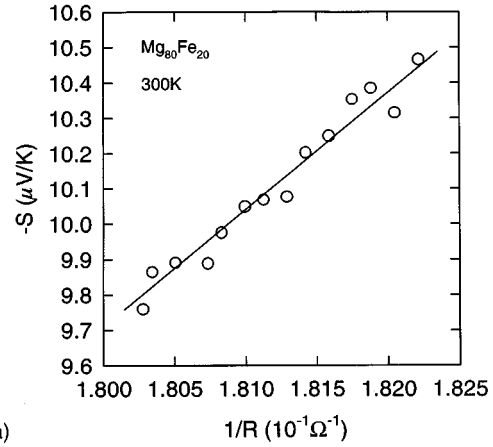
where  $S_0$  is the thermopower of the matrix and  $\beta = \rho_m / \rho_{AF}$  is the ratio of the matrix to total resistivity in zero field. The NG rule cannot be applied directly in the saturated limit, because spin-up and spin-down carriers have different resistivities. Either direct calculation from the Mott formula or application of the NG rule to each spin subband followed by appropriate addition<sup>14</sup> gives the following result:

$$\Delta S = \frac{\sqrt{\mathcal{R}}}{1 - \mathcal{R}} (1 - \mathcal{R} - \beta) (S_{\uparrow} - S_{\downarrow}) - \frac{\mathcal{R}\beta}{1 - \mathcal{R}} (S_{\uparrow} + S_{\downarrow} - 2S_0). \quad (15)$$

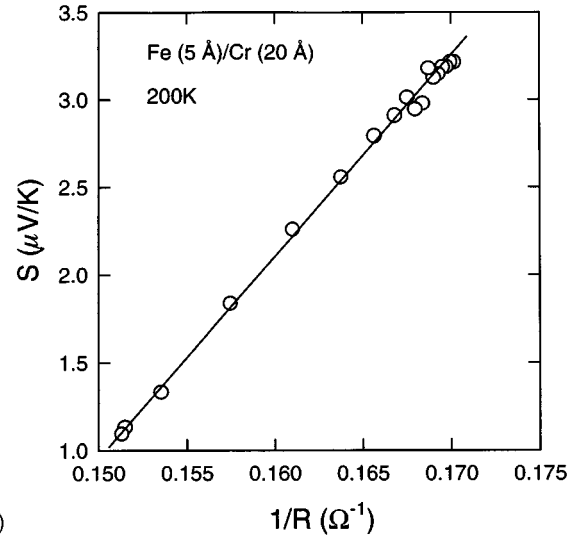
When the matrix resistance is negligible ( $\beta=0$ ), we recover Eq. (9).

If we assume that  $S_0$  is equal to the intrinsic TEP of the matrix material, the contribution of the matrix TEP to  $\Delta S$  can be estimated using Eq. (15). Because  $\rho_m < \rho_F$ , the maximum value of  $\beta$  is,  $\beta_{\max} = 1 - \mathcal{R}$ . Substituting this into Eq. (15) we see that the maximum contribution of the  $S_0$  term is  $-2\mathcal{R}S_0$  which is small for  $\beta \approx \beta_{\max}$ , typically less than 5–10 % of the observed value of  $\Delta S$ . This indicates that the large GMTEP and also the GMR must result from scattering into magnetic bands and not into the matrix-spacer layer bands.

In Eqs. (14) and (15) there are three unknown quantities ( $S_{\uparrow}$ ,  $S_{\downarrow}$ , and  $\beta$ ). Using the experimental values of  $\Delta S$  and  $\mathcal{R}$ , and  $S_{\uparrow} + S_{\downarrow}$  equal to the value for bulk Co, we have adjusted  $\beta$  to yield the observed zero-field thermopower for the AgCo sample. As seen in Table I, the asymmetry derivative is also very close to the bulk Co value  $\alpha' / \alpha = 2.5 \text{ eV}^{-1}$ . Kita *et al.*<sup>37</sup> have determined related expressions for multilayers, where the effect of the spacer layer is to provide a leakage path in parallel with the magnetoresistance. In this case,  $\beta$  measures the ratio of the leakage conductivity due to



(a)



(b)

FIG. 4. Plots of the thermopower vs conductance for samples of (a) granular MgFe and (b) Fe/Cr granular multilayer. The temperatures are indicated.

the spacer layer to the conductivity in the saturated state. Application of these formulae to a number of multilayers is also shown in Table I.

## V. THERMAL CONDUCTIVITY

The importance of inelastic scattering is a fundamental issue in understanding the source of the GMR effect. In principle, this can be determined from the applicability of the Wiedemann-Franz law but, in practice, it is usually difficult to separate electronic from lattice and magnon thermal conductivities. One method, usually applied to nonmagnetic metals, is to study the relationship between electrical and thermal magnetoresistances, the latter sometimes called the Maggi-Righi-Leduc effect.<sup>38</sup> For the systems of interest here, this method is particularly useful because the large negative changes in electrical resistance are mirrored in the thermal resistance and are almost certainly due to the same mechanism. This is advantageous since the background thermal leakages due to radiation, the conduction through sensor leads and any residual gas in the sample space, and the effect of the substrate and phonons are independent of magnetic field.

TABLE I. Properties of a number of Co-based and Co-like GMR systems. ML-2 is a sample found in Ref. 8. The quantity  $\beta$  is the ratio of matrix to demagnetized resistivities for the granular system, the ratio of spacer layer to saturated conductivities in the multilayers. Its value has been adjusted to bring observed and calculated TEP values into reasonable agreement. The partial thermopowers are fixed at  $S_{\uparrow} = -30 \mu\text{V/K}$  and  $S_{\downarrow} = -12 \mu\text{V/K}$ , their 300 K values for bulk Co, and are assumed to be linear in temperature. The 300 K matrix thermopower of the Cu-Ni alloy is taken to be  $-40 \mu\text{V/K}$  and that of pure Cu or Ag  $1 \mu\text{V/K}$ .

Material	$T$ (K)	$\mathcal{R}$	$\beta$	$S_d^{\text{obs}} (\mu\text{V/K})$	$S_s^{\text{obs}} (\mu\text{V/K})$	$S_d^{\text{calc}} (\mu\text{V/K})$	$S_s^{\text{calc}} (\mu\text{V/K})$
AgCo	100	0.14	0.41	-2.7	-3.0	-2.65	-3.0
Co/Cu(8.3 Å)	300	0.23	0	-19	-25.7	-16.7	-25.3
Co/Cu(8.3 Å)	100	0.28	0	-8.1	-11	-5.4	-8.6
Co/Cu(9.2 Å)	300	0.52	0	-19	-28.5	-14.5	-27.5
Py/Cu(10 Å)	300	0.18	0.1	-16	-20.9	-15.5	-20.4
Co/CuNi	300	0.06	0.18	-26	-28.1	-24.4	-26.4
ML-2	300	0.17	0.37	-11.5	-15.9	-12.2	-15.8
ML-2	79	0.31	0.22	-3.5	-5	-3.5	-5.3

Early measurements of the thermal conductivity of granular samples<sup>9</sup> and multilayers<sup>8</sup> demonstrated the presence of large negative magnetothermal resistance, which we abbreviate as GMTR. However, these studies did not report concurrent measurements of the GMR, which prevents a direct comparison of the two effects. We correct that deficiency here. Figure 5(a) shows the thermal conductance and electrical

resistance at 100 K of a AgCo granular sample, grown on Kapton. We use the Wiedemann-Franz law, Eq. (12), to write the thermal conductance in terms of the electrical resistance as

$$K(H, T) = TL_{\text{expt}}(H, T)/\gamma R(H, T) + K_0(T). \quad (16)$$

Here,  $R(H, T)$  is the electrical resistance;  $L_{\text{expt}}(H, T)$  is the experimental Lorentz number, which may depend on field and temperature;  $K_0(T)$  is the contribution from phonons, magnons, and the substrate, which we assume to have negligible field dependence; and  $\gamma$  is a geometrical factor that corrects for the different separations of the electrical and thermal contacts. (The electrical and thermal measurements were, as noted earlier, carried out simultaneously on two separate segments of the same sample. For this sample the geometrical factor is  $\gamma=0.6$ .) A test of this relationship is shown in Fig. 5(b), where it may be seen that the experimental Lorentz number is field independent. As Fig. 6 shows,  $L_{\text{expt}}$  is, within experimental uncertainty, independent of temperature and consistent with  $L_{\text{expt}} = (2.0 \pm 0.2) \times 10^{-8} \text{ W}\Omega/\text{K}^2$ , quite close to the free electron value. The tempera-

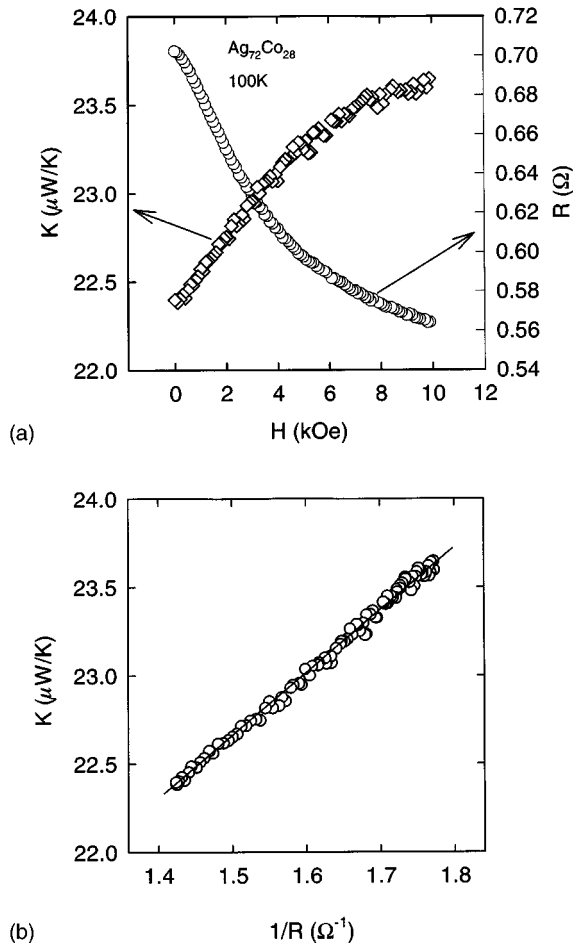


FIG. 5. (a) The thermal conductivity and electrical resistance of a granular AgCo sample vs applied field. (b) A test of the Wiedemann-Franz law on the same data.

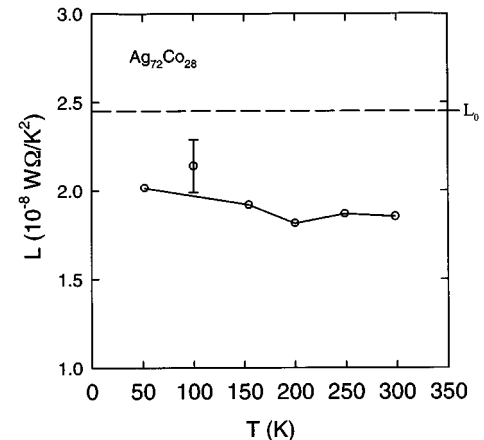


FIG. 6. The experimental Lorentz number for AgCo determined from the slope of curves such as that in Fig. 5(b). The datum at 100 K was taken after the sample was remounted. The dashed line marks the free electron value.

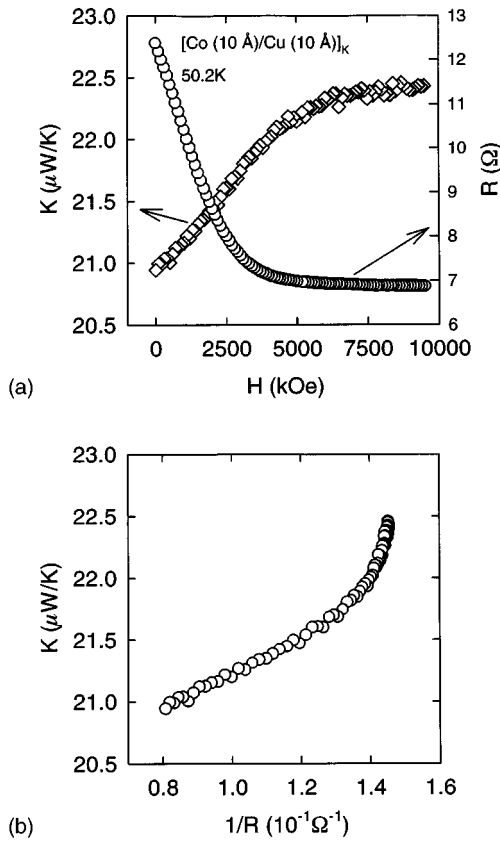


FIG. 7. (a) Thermal conductance and electrical resistance of a Co/Cu multilayer sample grown on Kapton vs applied field, measured at 50 K. (b) A plot of thermal vs electrical conductance with the field as an implicit variable. The nonlinearity reflects a failure of the Wiedemann-Franz law.

ture independence of  $L_{\text{expt}}$  suggests that the field-dependent electrical and thermal resistances are dominated by elastic scattering processes.

The electronic term in Eq. (16) comprises only 25% of the thermal conductivity at zero field and 100 K. At this temperature, the nominal thermal conductivity of the Kapton film is negligible. It is natural to assign this excess to the lattice thermal conductivity of the film. However, earlier measurements<sup>9</sup> on thick granular films reported that the electronic contribution was dominant. Either the process of removing the thick film from its substrate so cold-worked the sample that its lattice contribution was suppressed or the process of deposition has modified our Kapton substrates in a way that produces a much higher thermal conductivity. These two explanations need further investigation.

Similar measurements were performed on two multilayer samples  $[\text{Co}(10 \text{ \AA})/\text{Cu}(10 \text{ \AA})]_{\text{K}}$  and  $[\text{Co}(10 \text{ \AA})/\text{Cu}(23 \text{ \AA})]_{\text{K}}$  using the method described in Sec. III. The data taken at 50.2 K are shown in Fig. 7(a). Unlike the granular results, the thermal conductivity continues to increase at fields at which the electrical resistivity is essentially constant. This can be seen quite clearly in Fig. 7(b), where we plot the thermal vs electrical conductances. Unlike in granular samples,  $L_{\text{expt}}$  is now field dependent. It is temperature dependent as well: The Wiedemann-Franz law does not hold for the multilayer samples. The same effect may be seen on the second sample with the thicker Cu spacer, Fig. 8.

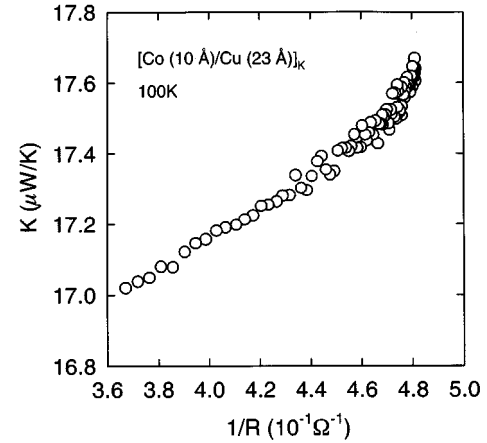


FIG. 8. Data similar to that of Fig. 7(a) taken on a Co/Cu multilayer with thicker Cu spacer layers. The failure of the Wiedemann-Franz law is evident.

In order to extract the field-dependent Lorentz number, we extrapolate the linear portion of the  $K(H, T)$  vs  $1/R(H, T)$ , generally valid for fields below 3.5 kOe. We then interpret the infinite-resistance intercept as lattice and substrate contribution  $K_0$  and subtract it from the data. The remaining thermal conductance is assumed to be entirely electronic, and the Lorentz number is calculated according to Eq. (16). While uncertainty in the extrapolated value is reflected in the magnitude of the effective Lorentz number, the field and temperature dependences are not affected. The results are shown in Fig. 9 for this sample, for which the geometric factor is  $\gamma = 0.045 \pm 0.006$ . For fields below 2 kOe, the values remain constant at each temperature. The failure of the WF law suggests that inelastic scattering may be more important in multilayers than in granular materials. Because multilayer samples can support low-energy magnons while small magnetic particles cannot, the possible involvement of spin waves is a reasonable starting point in seeking an explanation for the failure of the WF law. We return to this issue in Sec. VI B below.

## VI. DISCUSSION

### A. Thermoelectric power

Taken as a whole, the magnetothermoelectric power data appear to be consistent with the Mott scattering picture, in particular Eqs. (9) and (11). In all cases, changes in the resistivity are mirrored in the TEP so that TEP is proportional to the conductivity. This relationship, along with the magnitude of this effect, suggests that changes in the resistivity and TEP arise from a common cause. As was shown above, in the absence of spin-flip scattering, models in which the asymmetry ratio is constant in energy do not explain the observed GMTEP effect. The addition of matrix-spacer layer resistivity, as in Eq. (15), does not change this conclusion. This means the TEP data argue against the LZFM model, unless spin-flip scattering is included in the model.

By including spin-flip scattering, Pireaux *et al.* have argued that magnon absorption and emission leads to a difference in the TEP of the majority and minority bands.<sup>5</sup> This difference could be manifested in the GMTEP effect. As

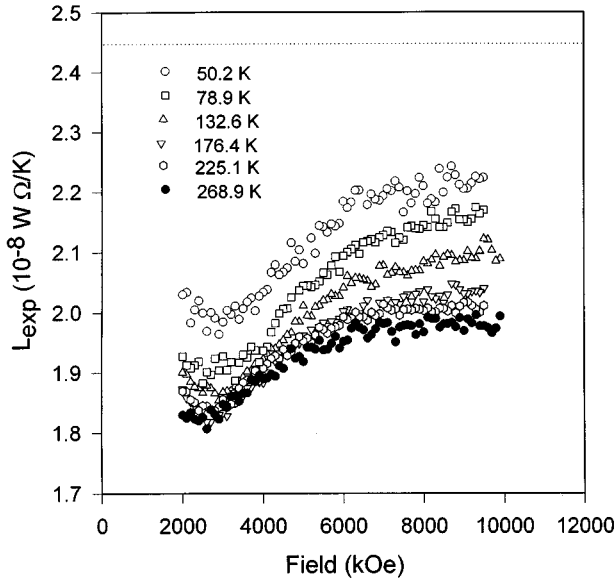


FIG. 9. The experimental Lorentz number  $L_{\text{exp}}$  vs magnetic field for the data shown in Fig. 7(b) along with that taken at other temperatures. Values were obtained from Eq. (16) using values of  $K_0$  extrapolated from the low-field portions of the  $K$  vs  $1/R$  curves.

was shown in the previous section, magnons can have a measurable effect on the transport properties of multilayers. Yet the GMTEP effect is also seen in granular systems where the magnon wavelengths are limited by the small size of the ferromagnetic granules. For typical Co granules (27 Å in diameter) the minimum magnon energy (assuming the bulk-like dispersion with no anisotropy gap) is  $\sim .01$  eV. Thus, in the temperature range used in these experiments, especially at lower temperatures, magnons should not effect the transport properties significantly. The constant Lorentz number of the granular samples attests to this. Models with an energy-independent asymmetry ratio that include spin-flip interactions therefore cannot account for the observed GMTEP effect in both multilayers and granular systems.<sup>9</sup>

In transition metals with dilute ferromagnetic impurities virtual bound states (VBS's) have been shown to account for the large, solute, and impurity-dependent TEP.<sup>32</sup> The existence of VBS at the magnetic/nonmagnetic interface has been suggested as the cause of the GMR and GMTEP.<sup>35</sup> While the VBS theory yields a scattering potential similar to Eq. (1), it differs from the conventional theory in that the VBS's are a result of resonant scattering. The LZFM model explicitly excludes resonant scattering. This resonance causes the impurity  $d$ -orbital DOS to factor into the spin-dependent scattering potential through  $s$ - $d$  hybridization. This leads to an asymmetry parameter which is energy dependent and equations for  $S_{\text{AF}}$  and  $S_{\text{F}}$  entirely equivalent to Eqs. (8). However, the VBS model is suspect for two reasons. First, the VBS contribution to the TEP is determined by the position and width of the impurity energy level compared to the Fermi energy so that the TEP of binary alloy systems that exhibit VBS's is typically quite different from either of the constituents. As shown in this work, magnetic multilayers typically have zero field TEP very close to that of the ferromagnetic component. In granular systems the situation is more complicated as we will discuss below. The second

problem with the VBS model is in the sign of the GMTEP. For Co/Cu multilayers, Inoue *et al.* predict  $\Delta S \equiv S_{\text{AF}} - S_{\text{F}} < 0$  while we observe a positive value.

There are some unresolved issues. One is the zero-field value of the TEP of granular systems. In multilayers, the zero-field value of the TEP is close to that of the ferromagnetic material as would be expected in the Mott scattering picture given above. This suggests that the interface scattering into the magnetic layers dominates the TEP as well as the resistivity. However, in granular materials where scattering in the matrix is important, the zero-field TEP differs from that of the ferromagnetic material (as in AgCo) and even may be of a different sign (as in MgFe). While we have discussed the effect of the matrix scattering as if the matrix should have the TEP intrinsic to the nonmagnetic material, this is probably not the case (especially in unannealed samples). Even small concentrations of ferromagnetic materials dissolved in a nonmagnetic material can have a large effect on the zero-field TEP and even cause the TEP to be field dependent.<sup>32</sup> This is due to the contribution to the TEP from VBS's. However, as the size of the magnetic clusters increases there should be a crossover from a situation where the TEP is dominated by scattering into VBS's to a situation where the TEP is dominated by scattering into bulk ferromagnetic bands. The MgFe system may be a good example. In the as-prepared state, magnetization and small-angle x-ray scattering measurements indicate that the majority of Fe exists in small ( $10\mu_B$ ) particles. These unannealed samples have a zero-field room-temperature TEP of  $-9.7 \mu\text{V/K}$  which is less than either bulk Fe ( $+15 \mu\text{V/K}$ ) or bulk Mg ( $-1.0 \mu\text{V/K}$ ). Upon annealing at 228 °C for 1 h, the small Fe particles precipitate out of the matrix, form large ( $250 \mu_B$  or more) Fe clusters, and the zero-field room-temperature TEP is changed to  $+1.20 \mu\text{V/K}$ . Although the analysis here is very qualitative, it is clear that when there is a large matrix contribution to the resistivity, a more detailed picture of the various scattering mechanisms is required to accurately determine the zero-field value of the TEP especially in granular systems where the band structure of very small ferromagnetic granules differs from the bulk.

Another problem with the Mott scattering picture is its inability to explain the observed temperature dependence of the GMTEP of Fe/Cr multilayers where the *sign* of the GMTEP effect changes with temperature. Our data on the Fe(50 Å)/Cr(20 Å) sample are in qualitative agreement with observations first made by other groups.<sup>3,5</sup> However, we note that we did not observe a sign change in the GMTEP of Fe/Cr granular multilayers. At present we have no explanation for this and more detailed work must be done.

## B. Thermal conductivity

As noted above, the Wiedemann-Franz ratio of transition metals drops dramatically below the Curie temperature. Kasuya<sup>24</sup> and, subsequently, Colquitt<sup>25</sup> attributed this drop to the effectiveness of magnons in thermally relaxing the conduction electron distribution. In both descriptions, however, only inelastic magnon scattering was considered, and detailed balance arguments eliminated the distinction between magnon creation and magnon annihilation. In the present situation, however, we argue that elastic scattering processes

dominate, but that magnon scattering opens a path for thermal relaxation that reduces the effective Lorentz number. We present here a simple model that illustrates how low-angle magnon processes can produce the effects observed in Fig. 9.

We consider the ferromagnetic configuration and write the rate at which spin-up electrons can be scattered into the spin-down (minority) band of one of the ferromagnetic layers. This occurs through the absorption of a magnon of wave vector  $Q = |k_{F,s} - k_{F,d}|$ , that connects  $s$  and  $d$  segments of the Fermi surface. This is presumably a small-angle process that affects mainly the thermal relaxation. Consequently, within the context of Fermi's golden rule, we can write a relaxation rate for this process as

$$W_F(k_{s\uparrow} \rightarrow k_{d\downarrow}) = 2G^2 \langle n_Q \rangle g_{\downarrow}(E_F) \quad (17)$$

and, similarly, for spin-down electrons,

$$W_F(k_{s\downarrow} \rightarrow k_{d\uparrow}) = 2G^2 \langle n_Q + 1 \rangle g_{\uparrow}(E_F). \quad (18)$$

There are two key differences between the two rates: (i) The spin-up rate depends on the presence of thermally excited magnons, while the spin-down rate involves magnon creation, and (ii) the densities of states are in the ratio  $\alpha$  given by Eq. (13a). In both cases,  $G$  is a matrix element of the  $s$ - $d$  exchange interaction and  $\langle n_Q \rangle$  is the Bose factor for magnons of wave vector  $Q$ .

The situation for antiferromagnetic alignment is quite different, as spin-up electrons (defined relative to one of the neighboring magnetic layers) can scatter by both magnon creation and annihilation processes. The rates for both spin channels are the same and can be written as

$$W_A(k_{s\downarrow} \rightarrow k_{d\uparrow}) = W_A(k_{s\uparrow} \rightarrow k_{d\downarrow}) \\ = G^2 g_{\downarrow}(E_F) \left[ \left( 1 + \frac{1}{\alpha} \right) \langle n_Q \rangle + \frac{1}{\alpha} \right]. \quad (19)$$

We assume that these rates add to the non-spin-flip scattering rates  $W_{i\uparrow}$  and  $W_{i\downarrow}$ , and that those are in the same ratio  $\alpha = W_{i\downarrow}/W_{i\uparrow}$  as the electrical resistivities. Defining  $\lambda = 2G^2 g_{\downarrow}(E_F)/W_{i\downarrow}$  and  $\mu = \lambda \langle n_Q \rangle$ , we can write the effective Lorentz numbers in the ferromagnetic and antiferromagnetic states as

$$L_F = L_0 \alpha \left( \frac{1 + \mu + \lambda/(1 + \alpha)}{(1 + \alpha\mu)(\alpha + \lambda + \mu)} \right), \quad (20)$$

$$L_{AF} = \frac{L_0}{1 + \mu + \lambda/(1 + \alpha)}. \quad (21)$$

We have assumed that the magnon scattering involves low-angle processes that do not affect the resistivity.

At sufficiently low temperatures, the magnon absorption will be frozen out; i.e.,  $\mu \rightarrow 0$ . In this limit the effective Lorentz numbers are in the ratio  $L_F/L_{AF} = [1 + \lambda/(1 + \alpha)]^2/[1 + \lambda/\alpha]$ . For the lowest-temperature data in Fig. 1, this ratio is 1.1 and  $\alpha \approx 3$  ( $\mathcal{R} = 0.25$ ), suggesting  $\lambda \approx 0.6$ . It is not possible to make a complete model, as the inelastic scattering rate is also temperature dependent. However, examination of Eqs. (20) and (21) will show that  $L_F$  is considerably more sensitive to changes in  $\mu$ , and is reduced as  $\mu$  increases, making it more temperature depen-

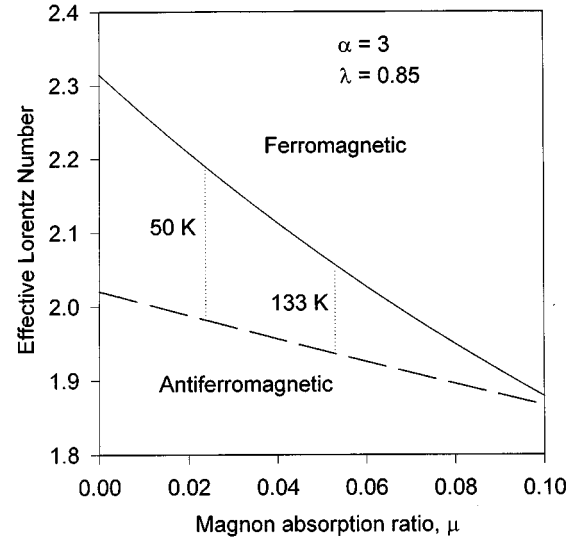


FIG. 10. Effective values of the Lorentz numbers for ferromagnetic and antiferromagnetic states in the magnon scattering model. The parameter  $\lambda$  is fixed here, although it is proportional to the inverse of the elastic scattering rate and therefore temperature dependent. The dotted lines indicate regions where the two effective Lorentz numbers match the data shown in Fig. 9.

dent, as observed. We demonstrate this in Fig. 10, in which  $L_F$  and  $L_{AF}$  are plotted as functions of  $\mu$  with the other parameters fixed at  $\alpha = 3$  and  $\lambda = 0.6$ .

## VII. CONCLUSION

We have presented data on the magnetic field dependence of the thermoelectric power and thermal conductivity for a variety of GMR systems, both multilayer and granular, and have proposed a model in which the scattering from the non-magnetic  $s$  bands into the magnetic  $d$  bands dominates the resistivity as well as the TEP. The majority of the data are in agreement with this model. The GMTEP effects measured are inconsistent with theories in which the spin asymmetry parameter  $\alpha$  is independent of energy even when spacer-layer or matrix scattering is included. We have also demonstrated that magnon scattering and impurity virtual bound states cannot explain the GMTEP effect in both granular and multilayer systems. While the TEP data do not rule out the contributions from nonresonant spin-dependent potentials to the GMR, the measurements demonstrate that the DOS of the ferromagnetic layer or granule must be included to properly explain the data.

The thermal conductivity in granular samples obeys the Wiedemann-Franz law, indicating that the scattering is elastic or large angle, while in multilayered samples the thermal conductivity shows significant deviations from the Wiedemann-Franz law, indicating a significant inelastic component. We ascribe this deviation to scattering from long-wavelength magnons. However, to explain the field and temperature dependence of the WF ratio, it is necessary that non-spin-flip processes be the dominant scattering mechanism.

While development of practical devices based on the GMR effect is proceeding by empirical methods, an elucidation of the mechanism that underlies the effect may provide

guidance for further improvements. We have argued here that the density of states at the ferromagnetic interface plays a dominant, if not essential, part in the GMR process. We are presently testing this assertion by systematic modification of the band structure of the ferromagnetic constituent. At the same time, a better theoretical understanding of the evolution of band structure at the interface between magnetic and non-magnetic metals would be, in our view, an important direction for future research.

## ACKNOWLEDGMENTS

The authors would like to thank Lei Xing and Y. C. Chang for their stimulating discussions and Kevin Roche, R. Ohigashi, D. Shimizu, M. Nishikawa, and Dr. Y. Sugita for assistance in sample growth. This research was conducted with financial support from DOE Grant No. DEFG02-91ER45439 at the University of Illinois, Materials Research Laboratory. The support of Mombusho through a Japanese Overseas Research Fellowship (E.K.) and a Distinguished Visiting Professorship (M.B.S.) is gratefully acknowledged.

- \*Present address: Physical Research Laboratory, Motorola, Inc., 2100 Elliott Rd., Tempe, Arizona 85226
- †Present address: IBM Almaden Research Center, 650 Harry Road, San Jose, California 95120-6099.
- <sup>1</sup>M. N. Baibich, J. M. Broto, A. Fert, F. Nguyen Van Dau, F. Petroff, P. Etienne, G. Creuzet, A. Friederich, and J. Chazalas, *Phys. Rev. Lett.* **61**, 2472 (1988).
- <sup>2</sup>B. Dieny, *J. Magn. Magn. Mater.* **136**, 335 (1994).
- <sup>3</sup>J. Sakurai, M. Horie, S. Araki, H. Yamamoto, and T. Shinjo, *J. Phys. Soc. Jpn.* **60**, 2522 (1991).
- <sup>4</sup>M. J. Conover, M. B. Brodsky, J. E. Mattson, C. H. Sowers, and S. D. Bader, *J. Magn. Magn. Mater.* **102**, L5 (1991).
- <sup>5</sup>L. Piraux, A. Fert, P. A. Schroeder, R. Loloee, and P. Etienne, *J. Magn. Magn. Mater.* **110**, L247 (1992).
- <sup>6</sup>J. Shi, R. C. Yu, S. S. P. Parkin, and M. B. Salamon, *J. Appl. Phys.* **73**, 5524 (1993); J. Shi, S. S. P. Parkin, L. Xing, and M. B. Salamon, *J. Magn. Magn. Mater.* **125**, L251 (1993).
- <sup>7</sup>J. Avdi *et al.*, *J. Appl. Phys.* **73**, 5521 (1993).
- <sup>8</sup>H. Sato, Y. Aoki, Y. Kobayashi, H. Yamamoto, and T. Shinjo, *J. Magn. Magn. Mater.* **126**, 410 (1993); H. Sato *et al.*, *J. Appl. Phys.* **76**, 6919 (1994).
- <sup>9</sup>L. Piraux, M. Cassart, J. S. Jiang, J. Q. Xiao, and C. L. Chien, *Phys. Rev. B* **48**, 415 (1993).
- <sup>10</sup>A. Fert and P. Bruno, in *Ultrathin Magnetic Structures II*, edited by B. Heinrich and J. A. C. Bland (Springer-Verlag, Berlin, 1994).
- <sup>11</sup>P. M. Levy, S. Zhang, and A. Fert, *Phys. Rev. Lett.* **65**, 1643 (1990); S. Zhang, P. M. Levy, and A. Fert, *Phys. Rev. B* **45**, 8689 (1992); S. Zhang and P. M. Levy, *J. Appl. Phys.* **73**, 5315 (1993).
- <sup>12</sup>D. M. Edwards and J. Mathon, *J. Magn. Magn. Mater.* **93**, 85 (1991); J. Mathon, *Contemp. Phys.* **32**, 143 (1991).
- <sup>13</sup>S. S. P. Parkin, *Phys. Rev. Lett.* **71**, 1641 (1993).
- <sup>14</sup>D. K. C. MacDonald, *Thermoelectricity: An Introduction to the Principles* (Wiley, New York, 1962), pp. 110–116.
- <sup>15</sup>L. Xing, Y. C. Chang, M. B. Salamon, D. M. Frenkel, J. Shi, and J. P. Lu, *Phys. Rev. B* **48**, 6728 (1993).
- <sup>16</sup>N. F. Mott and H. Jones, *The Theory of the Properties of Metals and Alloys* (Dover, New York, 1958).
- <sup>17</sup>S. S. P. Parkin, N. More, and K. P. Roche, *Phys. Rev. Lett.* **64**, 2304 (1990).
- <sup>18</sup>S. S. P. Parkin, *Phys. Rev. Lett.* **67**, 3598 (1991).
- <sup>19</sup>J. Q. Xiao, J. S. Jiang, and C. L. Chien, *Phys. Rev. Lett.* **68**, 3749 (1992); A. E. Berkowitz *et al.*, *ibid.* **68**, 3745 (1992).
- <sup>20</sup>A. Fert and I. A. Campbell, *J. Phys. F* **6**, 849 (1976).
- <sup>21</sup>J. Ziman, *Principles of the Theory of Solids* (Cambridge University Press, Cambridge, England, 1964).
- <sup>22</sup>J. L. Duvall, A. Fert, L. G. Pereira, and D. K. Lottis, *J. Appl. Phys.* **75**, 7070 (1994).
- <sup>23</sup>M. J. Laubitz, T. Matsumura, and P. J. Kelly, *Can. J. Phys.* **54**, 92 (1976).
- <sup>24</sup>T. Kasuya, *Prog. Theor. Phys. Jpn.* **22**, 227 (1959).
- <sup>25</sup>L. Colquitt, Jr., *Phys. Rev.* **139**, A1857 (1965).
- <sup>26</sup>S. S. P. Parkin, Z. G. Li, and D. J. Smith, *Appl. Phys. Lett.* **58**, 2710 (1991).
- <sup>27</sup>D. H. Mosca, F. Petroff, A. Fert, P. A. Schroeder, W. P. Pratt, and R. Laloee, *J. Magn. Magn. Mater.* **94**, L1 (1991).
- <sup>28</sup>S. S. P. Parkin, C. Chappert, and F. Herman, *Europhys. Lett.* **24**, 71 (1993).
- <sup>29</sup>R. Nakatani, T. Dei, and Y. Sugita, *Jpn. J. Appl. Phys.* **31**, L1417 (1992).
- <sup>30</sup>K. Pettit, E. Kita, K. Araga, A. Tasaki, and M. B. Salamon, *J. Appl. Phys.* **75**, 6918 (1994).
- <sup>31</sup>R. B. Roberts, *Philos. Mag.* **36**, 91 (1977).
- <sup>32</sup>F. J. Blatt, P. A. Schroeder, C. L. Foiles, and D. Greig, *Thermoelectric Power of Metals* (Plenum, New York, 1976).
- <sup>33</sup>J. Shi, E. Kita, S. S. P. Parkin, and M. B. Salamon, *J. Appl. Phys.* **75**, 6455 (1994).
- <sup>34</sup>J. Shi, E. Kita, L. Xing, and M. B. Salamon, *Phys. Rev. B* **48**, 16 119 (1993).
- <sup>35</sup>J. Inoue, H. Itoh, and S. Maekawa, *J. Phys. Soc. Jpn.* **61**, 1149 (1992).
- <sup>36</sup>M. C. Cadeville and J. Roussel, *J. Phys. F* **1**, 686 (1971).
- <sup>37</sup>E. Kita, J. Shi, K. Pettit, M. B. Salamon, R. Nakatani, Y. Sugita, and K. Hoshino (unpublished).
- <sup>38</sup>J. E. Parrott and A. D. Stuckes, *Thermal Conductivity of Solids* (Pion Limited, London, 1975).